Gold-Electroplating Technology for X-Ray-Mask Fabrication

by

Kenneth W. Yee

B.S., University of California at Berkeley (1990)

Submitted to the Department of Electrical Engineering and Computer Science
in partial fulfillment of the requirements for the degree of

Master of Science in Electrical Engineering and Computer Science

at the

MASSACHUSETTS INSTITUTE OF TECHNOLOGY

June 1996

© Massachusetts Institute of Technology 1996. All rights reserved.

Author ....
Department of Electrical Engineering and Computer Science
May 10, 1996

Certified by ....
Henry I. Smith
Joseph F. and Nancy P. Keithley Professor of Electrical Engineering
Thesis Supervisor

Accepted by ....
Chairman, Departmental Committee on Graduate Students

MASSACHUSETTS INSTITUTE OF TECHNOLOGY

JUL 1 6 1996 Eng.

LIBRARIES

Gold-Electroplating Technology for X-Ray-Mask Fabrication

by

Kenneth W. Yee

Submitted to the Department of Electrical Engineering and Computer Science
on May 10, 1996, in partial fulfillment of the
requirements for the degree of
Master of Science in Electrical Engineering and Computer Science

Abstract

A critical component of proximity x-ray lithography is the patterning of the absorber material on the x-ray mask. In this thesis methods and techniques have been advanced to diagnose and solve a problem with the gold-electroplating process developed in the MIT NanoStructures Laboratory for the purpose of patterning sub-0.1 μm absorber features on x-ray masks. Bright-field transmitted-light optical microscopy in conjunction with a "thickness standard" was used to measure the thickness of the plated-gold films. This method led to the diagnosis of a non-uniform gold-plating rate in which the gold film was "depleted" at resist edges. To further elucidate the origin of this defect, the electrochemistry of the plating solution was investigated. A means of characterizing the cathode voltages of the plating reaction as a function of plating-current density and brightener concentration was developed. The electrochemical study suggests that chemical contamination in the plating solution had occurred, either from use or initially from the manufacturer, and replacement of the solution was necessary. This study also reveals that the composition of uncontaminated plating solution varies with time as a result of the oxidation of a brightening additive to the solution.

Thesis Supervisor: Henry I. Smith
Title: Joseph F. and Nancy P. Keithley Professor of Electrical Engineering

Acknowledgments

I'd like to express my sincere thanks to the many people who have helped me through to the end of my thesis and enlivened my experience at MIT and in graduate school.

Special thank-yous to those people with whom I've shared many moments kvetching about life and/or graduate school, and to those who have helped me out during the crunch times: Kathy Chen, Ray and Julie Ghanbari, Kathy Krisch, John-Paul Mattia, Lisa Su, Terry Talbot, Caroline Tio, Lisa Wang, and Albert Young. I can hardly hope to repay my karmic debts to you here, but JP has sagely informed me that the thing about karmic debts is that they can be paid back to just about anyone, anywhere. Special thanks to Elaine Chew, Leonard Lublin, Andrew Berger, Kristie Bosko, Lauren Crews, and Aaron Brandes.

Thanks to Liz Galvan, Risa Nesselroth, and Marg Blakeney for the many illuminating thoughts that we've shared over email. Who would have thought that luminous prose on screen could be so valuable?

Many thanks to my buddies from those heady, youthful days at Cal: Heidi Okamura, Jim Kinoshita and Jean Cho, Bruce Reznik, Eric and Lisa Lindquist. Thanks also to Ceci Flinn, Mike Trevino, Neal Dorow for making the Alumni Club here so enjoyable! Go Bears!

I'd like to express my gratitude to my sister, Amy Yee, and her husband Eric Paulson, and their kids, Benjamin and Christopher, for the many relaxing weekends, and for the enjoyable moments in babysitting as well. Thanks to my brother, Gene, for all of the frequent-flier tickets he provided me (they were put to good use!). Thank you to his wife Jennifer and their son Joshua, too!

Many thanks to Martin Burkhardt, Vincent Wong, Mark Schattenburg, Bob Fleming and Irv Plotnik with whom we shared many discussions and lab hours working on gold electroplating. Many thanks also to Raul Acosta of IBM, Bill Dauksher and Doug Resnick of Motorola for technical advice, comments, and discussions.

Much gratitude is owed to many other students with the NSL and the MTL community. Among those I've had the distinct pleasure of working with and learning

from: Tony Yen, Bill Chu, Isabel Yang, Yao-Ching Ku, Satyen Shah, Scott Hector, Jim Hugunin, Arvind Kumar, Hang Hu, Alberto Moel, Michael Lim, Gee Rittenhouse, and Kathy Early.

Again, an incalculable debt is owed to the staff of the NSL: Jimmy Carter, Mark Mondol, Jeannie Porter, Bob Sisson. Thank you for keeping everything running in tip-top shape through the appropriate combination of subtle manipulation and brute force, and the occasional bit of miracle work.

Thank you, to my advisor Professor Hank Smith. Thanks also to Professors Dimitri Antoniadis and Terry Orlando. Thank you for all of your guidance, your patience, and for presenting yourselves as examples of how good research is done.

Special thanks go to my Uncle Sinclair and Aunt Genevieve Yee especially for the guidance and support and love in the final stages of the thesis writing.

Finally, thank you to my parents, Robert and Sim Yee, for all of the love and support they've given me. Without them, none of this would be possible.

Contents

Abstract **2**

Acknowledgments **4**

List of Figures **9**

1 Introduction **11**

1.1 X-Ray Lithography Overview 11

1.1.1 X-Ray Masks 12

1.1.2 Overview of Mask-Fabrication Process 12

1.2 Difficulties Encountered 14

2 Diagnosis of Plating Defects **17**

2.1 Motivation 17

2.2 Transmitted-Light Optical Microscopy 20

2.2.1 Observation of "Edge-Depletion" Defects 22

2.2.2 Flex-Glass Substrates 24

2.2.3 Observation of "Bubble" Defects 25

3 Electrochemistry of Gold Plating **29**

3.1 Introduction 29

3.2 BDT-510 Plating Solution Chemistry 29

3.3 Reference Electrode 31

3.3.1 Hull-Cell Measurements 32

3.3.2 In-situ Measurement 35

3.4 Experimental Results 35

3.4.1 Varying Concentration of BDT Brightener 35

3.4.2 Age of Plating Bath 37

3.4.3 Measurement of Defective Bath 37

3.5 Discussion of Measurements 40

4 Conclusions **41**

Bibliography **43**

List of Figures

1-1 Photograph of the NSL mask blank [9]. The silicon-nitride membrane is 31 mm in diameter. 13
1-2 Process flow for x-ray-mask replication. 15

2-1 Schematic illustration of the top views of a (a) defective "daughter" mask and (b) its corresponding mother mask. The fine feature on the "daughter" mask is absent. (The polarity reversal occurs when positive resist is used for the replication of the "mother" onto the "daughter" mask.) 18
2-2 An example of a sample with a uniform plating rate between coarse and fine gold features. The gold thickness is 700 nm, the linewidth is 100 nm. 19
2-3 Transmitted power as a function of wavelength through a 200-nm-thick gold film on top of a 1-μm-thick silicon nitride membrane. [10] . . . 21
2-4 Illustration of "edge-depletion" defects as viewed (a) in an optical microscope using transmitted-light illumination. (b) Possible cross-section that would result in (a). 23
2-5 SEM photo of a possible bubble defect of diameter $\sim$0.5 μm. 26
2-6 Illumination set up to attempt direct observation of bubble evolution. 27

3-1 Illustration of potential distribution in a typical electroplating reaction 31
3-2 Schematic of plating circuit illustrating SCE placement 32
3-3 Illustration of a Hull plating cell. The geometric configuration of the Hull cell dictates the current-density distribution at the cathode. . . . 33

3-4 Cathodic potential, as measured by SCE, versus anode current for BDT-510 for varying BDT Brightener concentrations 34
3-5 Family of curves for the cathode voltage versus current density for varying BDT Brightener concentration. 36
3-6 Cathode potential versus current density for different plating-bath ages. The concentration of BDT Brightener at 0 weeks is 5 ml/gallon. . . . 38
3-7 Measurement of the cathode potential versus current density for the defective plating bath. For comparison, the corresponding measurement for plating baths with 0 and 5 ml/gal concentrations of BDT Brightener are also shown. 39

Chapter 1

Introduction

1.1 X-Ray Lithography Overview

With the desire for increased computing ability, there is a demand for increasing the density per unit area of devices on integrated-circuit chips. This requires the technology to fabricate devices with fine feature sizes and low defect density, and under strict design tolerances.

Proximity x-ray lithography, first demonstrated in 1971 [1], is a technology capable of producing feature sizes under 0.1 μm. It has many advantages for this application. The wavelengths for soft x-rays (λ from 0.5 nm to 40 nm) are smaller than minimum feature sizes for most devices. Compared to deep-UV optical projection lithography, proximity x-ray lithography offers a large depth of field, so that the effects of substrate topography on lithography are minimized. Furthermore, since most materials have an index of refraction of approximately 1 at x-ray wavelengths, scattering phenomena (due to substrate composition or spurious dust particles) are minimized. Thus, proximity x-ray lithography is, in principle, capable of producing fine, submicron features with vertical sidewalls in a single-layer resist scheme, independent of substrate composition and topography.

Proximity x-ray lithography is also desirable with respect to manufacturing requirements. Because x-ray lithography is essentially "shadow casting" at x-ray wavelengths, the dependence on complicated optical systems with large fields of view is

minimized. Furthermore, x-ray lithography is a parallel process, thus making it desirable in terms of increased throughput.

Proximity x-ray lithography is a highly desirable technology for the fabrication of microelectronic devices, especially those that take advantage of small feature sizes, such as quantum-effect devices (e.g. coulomb-blockade devices [2], planar resonant-tunneling field effect-transistors (PRESTFETs) [3], [4], grid-gate transistor structures [4]), opto-electronic devices (e.g. distributed-feedback lasers [5]), and deep-submicron MOSFETs [6].

A critical component of this technology is the perfection of the x-ray mask. Because x-ray lithography is a proximity-printing technology, the absorber features on the mask must be patterned to the same size as the features desired on the final substrate. This presents a considerable technical challenge in fabricating the x-ray masks. The MIT NanoStructures Laboratory (NSL) has expended considerable effort towards the development of x-ray masks. The current mask configuration will be described in the next section.

1.1.1 X-Ray Masks

The x-ray mask blank used by the NSL consists of a 31-mm-diameter silicon-nitride membrane supported by a silicon "mesa" ring anodically bonded to a Pyrex frame (Figure 1-1) [7], [8]. The details of the fabrication are given in [9].

Gold is used as an absorber material for the x-ray mask. As discussed in [9], the gold is patterned onto the mask by means of an electroplating procedure. In order to plate the gold onto the x-ray mask blank, a plating base of a 50 Å-thick nichrome adhesion layer followed by a 100 Å-thick gold seed layer is electron-beam evaporated onto the mask blank.

1.1.2 Overview of Mask-Fabrication Process

We wanted to make an x-ray mask with sub-0.1-μm linewidths, using the process developed by the NSL. This process is outlined below. The full details are discussed

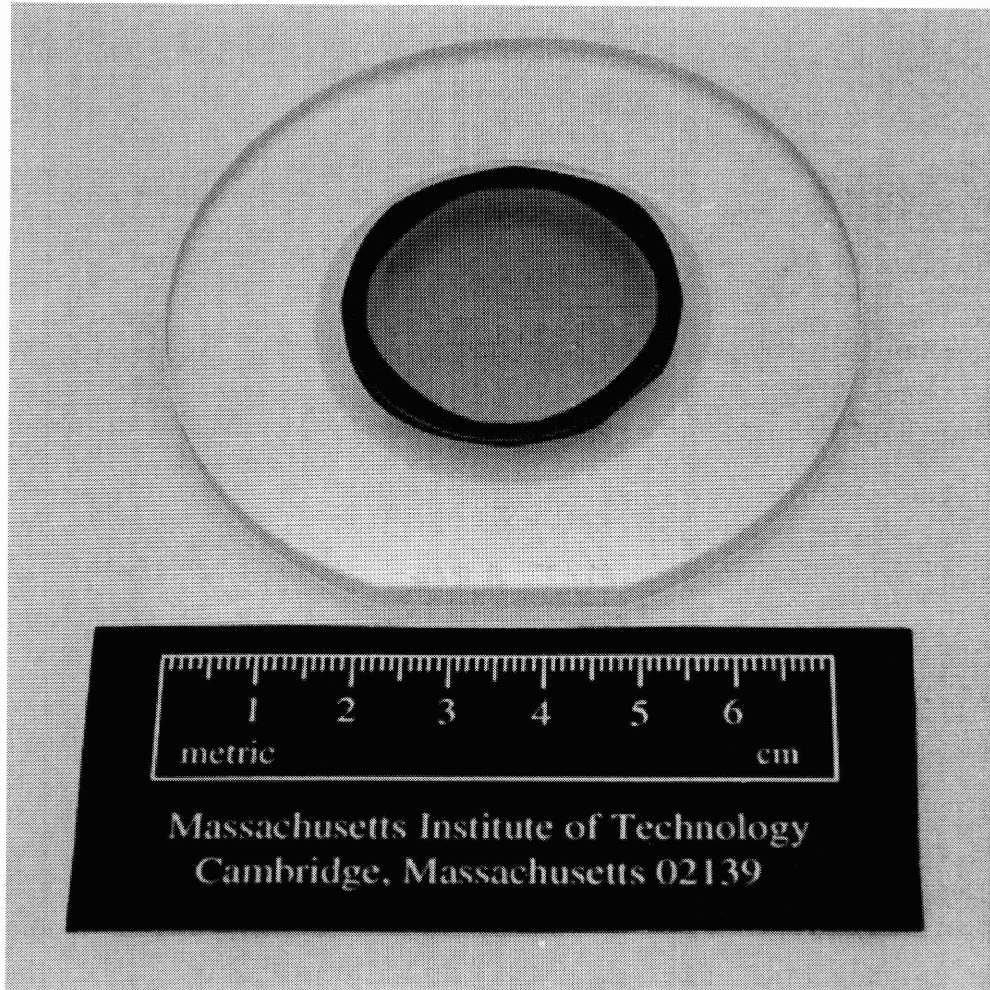

Figure 1-1: Photograph of the NSL mask blank [9]. The silicon-nitride membrane is 31 mm in diameter.

in [9].

1. Coat mask blank with poly-(methyl-methacrylate) (PMMA). This will be the "mother" mask.

2. Write this "mother" mask using scanning electron-beam lithography (SEBL). (Figure 1-2(a))

3. Develop PMMA.

4. Plate gold onto the "mother" mask, using the PMMA as a mold, strip PMMA. (Figure 1-2(b))

5. Evaporate gap-setting studs. (Figure 1-2(c))

6. Coat mask blank with PMMA. This will be the "daughter" mask.

7. Expose the "daughter" mask with the "mother" mask using the NSL's electron-bombardment x-ray source. (Figure 1-2(d))

8. Develop PMMA.

9. Plate gold on the "daughter" mask, strip PMMA. (Figure 1-2(e))

10. Strip PMMA.

1.2 Difficulties Encountered

In attempting to follow the process for X-ray mask-fabrication, we encountered difficulties printing fine features from the "mother" mask onto the "daughter" mask during the x-ray exposure.

As much of our work depended on having viable "daughter" masks for device exposures, it was necessary to determine the origin of the difficulties and to improve the existing process to resolve these fabrication issues. The approach we took was first to identify the problem and then to understand its origin by using analytical tools and

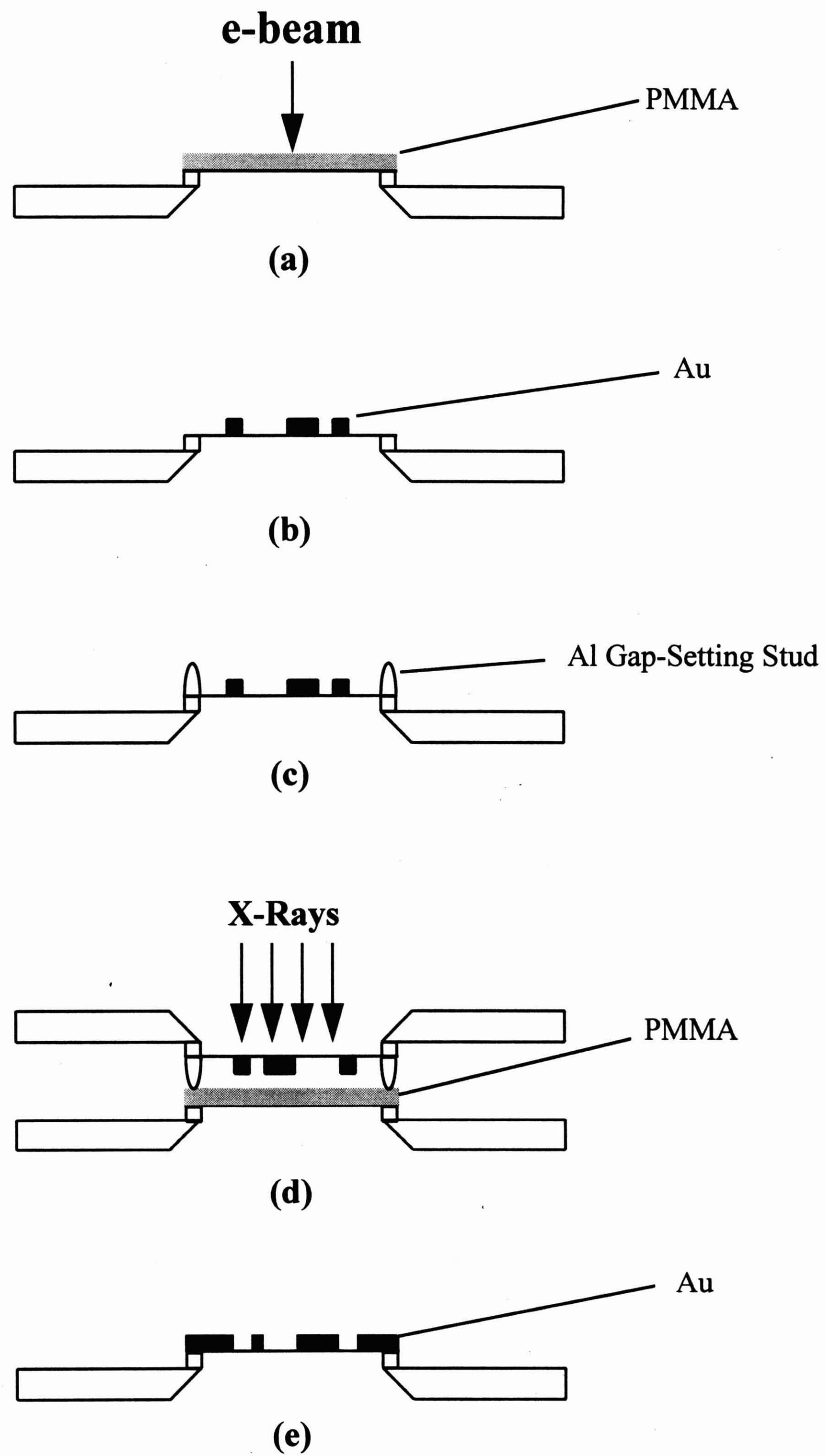

Figure 1-2: Process flow for x-ray-mask replication.

methods that we developed. The findings presented in this thesis indicate that the problems with the mask fabrication were likely the result of chemical contamination of the plating bath, either in the initial bath received from the vendor or through usage.

In Chapter 2 the diagnosis of our mask problems will be presented. By inspecting our plated masks using bright-field transmitted-light optical microscopy, we determined that our problems with replicating the "mother" mask onto the "daughter" mask were due to a non-uniform gold-plating rate near the edges of the PMMA features. Fine features would plate at a slower rate than coarse features. As a result, the fine gold features on the "mother" mask were too thin to provide sufficient contrast in the subsequent x-ray exposure to print the corresponding features onto the "daughter" mask. A possible cause for this "edge-depletion" defect was suggested by the observation of bubble-like defects on other plated samples.

Chapter 3 describes experiments to understand the plating solution and its associated additives electrochemically. There is some evidence that the "edge-depletion" defect is related to undesired chemical reactions occurring in the plating solution. We also observed that the electrochemical behavior of uncontaminated plating solution changes as the solution "ages."

Finally, some preliminary conclusions will be presented in Chapter 4, as well a summary of ongoing work.

Chapter 2

Diagnosis of Plating Defects

2.1 Motivation

Problems were observed in the mask fabrication process when transferring device patterns from the "mother" mask onto the "daughter" mask. Typically, the larger features would be transferred as expected, but the fine-features (e.g. sub-0.1 μm gate fingers) would not. A schematic illustration of this is shown in Figure 2-1.

On the "daughter" mask, the gold was plating as if the fine features on the "mother" mask had failed to adequately absorb the exposing x-rays during the "mother"-"daughter" exposure. The absence of a fine gold space on the "daughter" mask is indicative that the PMMA mold for the gold-plating on the "daughter" mask did not correspond to the gold patterns on the "mother" mask, as the fine gold features on the "mother" mask had failed to transfer to the PMMA on the "daughter" mask.

Initially, diffraction effects during the x-ray lithography step and loss of PMMA adhesion during mask processing were investigated as a possible cause of the pattern-transfer problem. However, these were ruled out for reasons presented below:

1. Diffraction effects

   Because the mask-replication exposure is a microgap exposure, the gap spacing between the "mother" mask and the "daughter" mask is critical. If the gap spacing is greater than a certain distance, diffraction may result in a low-

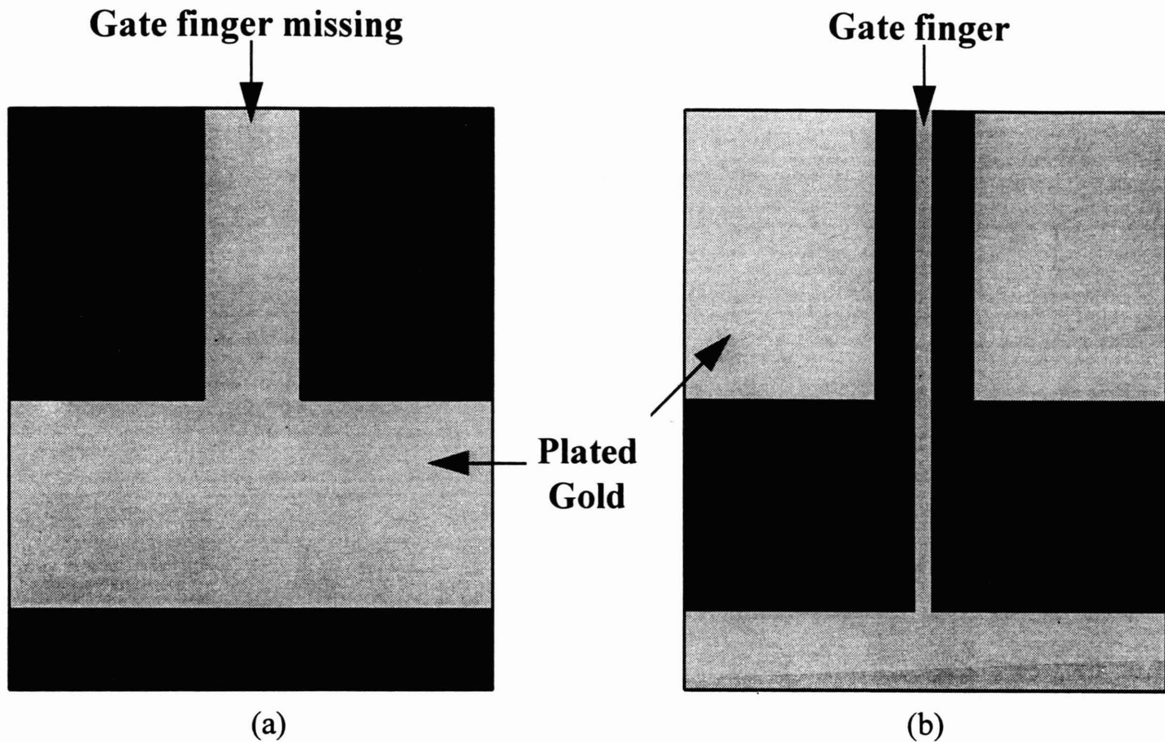

Figure 2-1: Schematic illustration of the top views of a (a) defective "daughter" mask and (b) its corresponding mother mask. The fine feature on the "daughter" mask is absent. (The polarity reversal occurs when positive resist is used for the replication of the "mother" onto the "daughter" mask.)

contrast exposure, and the fine features may not be replicated accurately onto the "daughter mask." When the defective "daughter" masks were exposed, the gap between "mother" and "daughter" mask was measured to be well under the maximum allowable gap according to $g = \alpha w^2/\lambda$, using $\alpha \sim 1$, x-ray wavelength $\lambda = 1.3$ nm, minimum resolvable linewidth $w = 0.1$ μm, and assuming 10db x-ray attenuation in the absorber. This simple calculation yields a maximum gap spacing of $\sim$7 μm for resolving a 0.1-μm-wide line, while the observed gaps used during the exposures were on the order of 1 μm or less. Diffraction effects were not likely to be the cause of the replication problems.

2. PMMA feature loss during the processing of the "daughter" mask

At various times during the development of the "daughter" mask, the sample was inspected in an optical microscope, and the fine features were not visible

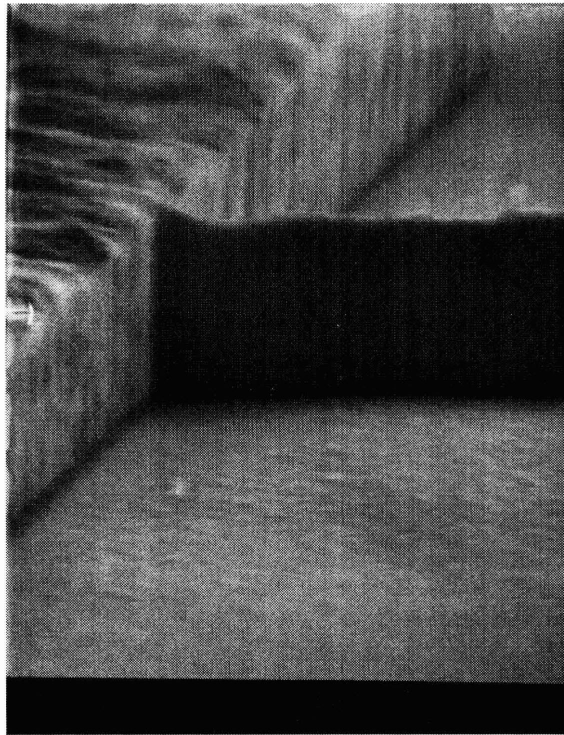

Figure 2-2: An example of a sample with a uniform plating rate between coarse and fine gold features. The gold thickness is 700 nm, the linewidth is 100 nm.

in the resist. This immediately suggests that the loss of PMMA features due to indelicate processing is not occurring, as the fine features were absent even in partially developed samples.

Since the replication problem seemed to be caused by an x-ray exposure problem, the possibility of a non-uniform plating rate between coarse and fine features was considered. If the fine features on the mother mask plate at a slower rate relative to the plating rate of the larger features, then the fine gold features would not be of sufficient thickness to provide the 10db contrast needed for the exposure. Normally, this is not to be expected, and Figure 2-2 is a SEM micrograph of a sample that demonstrated a uniform plating rate between coarse and fine features. But we decided to explore the possibility of non-uniform plating rates more thoroughly. The findings will be presented and discussed in Section 2.2.

At the same time, a study of the electrochemical properties of the plating reaction was made to explore the possibility that the chemistry of the plating solution might

be leading to defective gold films. This will be discussed in Chapter 3.

2.2 Transmitted-Light Optical Microscopy

Bright-field transmitted-light optical microscopy is used to determine whether the electroplated-gold film on an x-ray mask is sufficiently thick to provide the requisite contrast for subsequent x-ray exposures. For Cu_L x-ray lines (1.3-nm wavelength), a gold-film thickness of 200 nm is required to provide 10 dB contrast between open regions and plated regions on the x-ray mask. By inspecting the transmission of optical light through a plated region and comparing to the transmission of a "thickness standard," (an x-ray mask membrane with various thicknesses of gold electron-beam evaporated upon it) the thickness of the plated film is determined to within the gradations in thickness of the gold films on the thickness standard.

One's choice in selecting the type of light source for the optical microscope is dictated by the thickness of the gold film and its optical properties. Over most optical wavelengths, the skin depth of a gold film is on the order of nanometers, so one would expect a 200-nm-thick film of gold to be opaque over visible wavelengths (range of λ from 0.4 to 0.8 μm). However, a careful consideration of tabulated index-of-refraction data reveals a transmissive peak in green light (wavelength roughly 0.5 μm) (Figure 2-3. This transmissive peak in the green allows the use of the optical microscope with conventional light sources for rough comparisons of gold-film thickness.

With conventional microscope light sources, the amount of light transmitted through 200 nm of gold is barely discernable to the naked eye. In principle, the comparison may also be done electronically by capturing the microscope image with a CCD camera and correlating gray levels to thicknesses. In addition, a brighter light source such as a laser may also be used to increase the discernable signal through 200-nm-thick films, or for thicker films.

The gold-thickness standard was prepared from an x-ray mask with the standard plating base of 5 nm of NiCr and 10 nm Au evaporated onto the membrane. Various thicknesses of gold (0, 100, 150 and 200 nm) were electron-beam evaporated onto

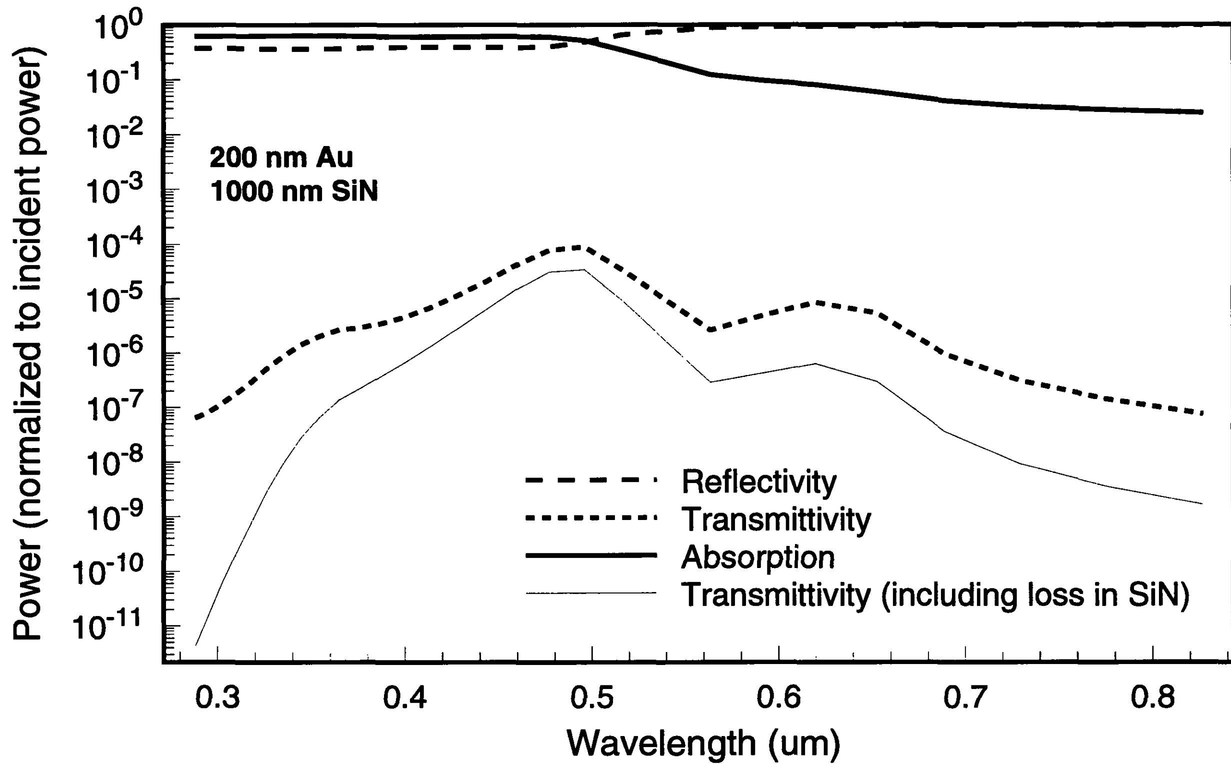

Figure 2-3: Transmitted power as a function of wavelength through a 200-nm-thick gold film on top of a 1-μm-thick silicon nitride membrane. [10]

this mask, by progressively opening the shutter to the evaporated-gold source and exposing a larger area of the mask membrane at each evaporation step.

The thickness of the plated film may be determined to within the thickness gradations on the thickness standard. This is done by comparing the observed intensity of transmitted light through the plated-gold film on an x-ray mask with the intensity of the transmitted light through the thickness standard. Typically, it is sufficient for the plated-gold film to transmit less light than the 200-nm-thick region on the thickness standard to insure 10 dB contrast at Cu_L wavelengths.

In order for a thickness standard to be reliable in determining the plated-gold-film thickness optically on an x-ray mask, the membranes of both mask and standard must have the same optical transmittivity, and they both must have the same thicknesses of plating-base metals. Thickness standards appropriate for different types of mask samples may be prepared, for example, with a nonstandard plating base.

2.2.1 Observation of "Edge-Depletion" Defects

When inspecting an x-ray mask with a 200-nm-thick plated-gold film in a transmitted-light bright-field microscope, the plated regions should be virtually opaque using conventional transmission illumination. By using a sub-stage condenser, the region of illumination may be apertured down to a small area to facilitate this type of transmission inspection.

The "problematic" masks (i.e. "mother" masks with patterns that could not be reliably transferred onto the "daughter" masks) were inspected using the substage condensor. When the area of illumination was aligned within the edge of a plated-gold feature, a variation of brightness was observed, as illustrated in Figure 2-4. The observed spot was brighter near the edge of the feature. This bright region would taper away from the edge with a length scale on the order of micrometers. By comparing the brightness of the spot near the edge of the feature to a thickness standard, we concluded that the gold film near the edge of the resist mold was thinner than the gold film in the "bulk" region of the feature. In one case, the thickness was estimated to be approximately 100 nm, a factor of 2 thinner than the bulk thickness of 200 nm.

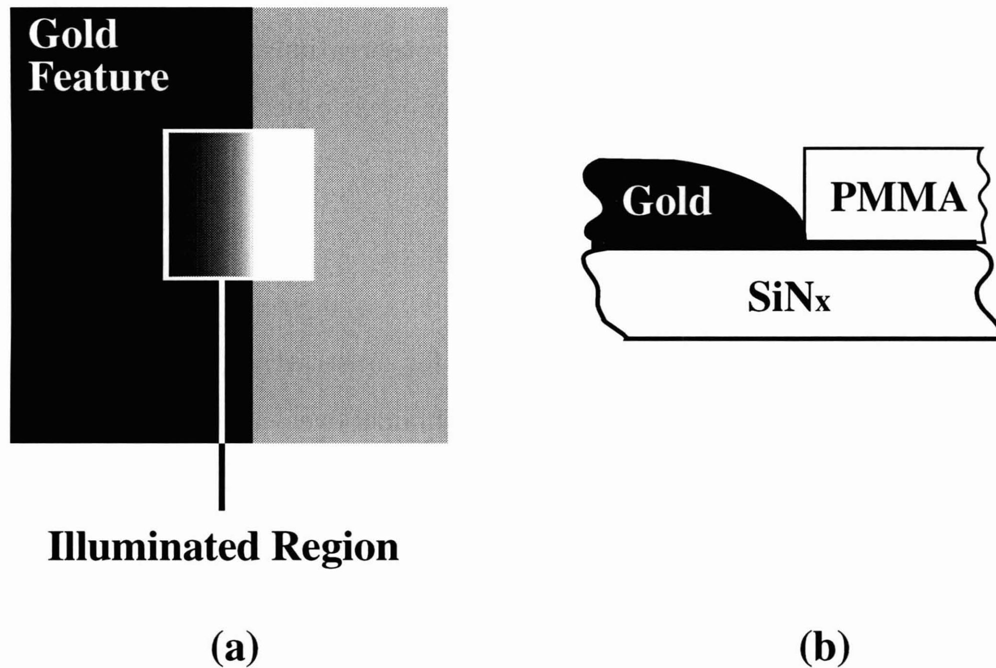

Figure 2-4: Illustration of "edge-depletion" defects as viewed (a) in an optical microscope using transmitted-light illumination. (b) Possible cross-section that would result in (a).

The use of bright-field transmitted-light optical microscopy is limited to features that can be resolved, sizes on the order of 0.5 μm. With conventional sub-stage illumination and condensing and an appropriate thickness standard, measureable thicknesses are limited to 200 nm or less. In principle, a brighter light source such as a laser may be used to measure thicker films (or to increase the spot intensity through 200-nm-thick films). The use of laser illumination may yield spurious intensity variations near the edges of plated features due to diffraction phenomena [11].

Transmitted-light microscopy with a substage condenser are used to measure the thickness and plating rate of the gold features on an x-ray mask. Operationally, a mask is plated for half of the time required to obtain the desired thickness based on a previous rate. The thickness is determined by using the optical microscope and a thickness standard, and the plating rate is recalibrated. The remainder of the film is then plated. Inspection by optical microscopy is non-contact and thus poses minimal

risk to the silicon-nitride membrane. It is preferable to a previous method using a profilometer to measure the step height between the resist mold and the region onto which the gold is to be plated. Profilometer observations of edge-depletion defects may also be obscured by noise, as the membrane is especially sensitive to ambient vibrations.

2.2.2 Flex-Glass Substrates

Previously, samples were limited to silicon-wafer substrates or x-ray mask-blank substrates. The advantage of using x-ray mask blanks over silicon-wafer substrates for plating experiments is the ability to inspect plated samples using transmitted-light illumination, due to the optically transmissive membrane onto which the gold films are plated.

The films plated onto opaque silicon-wafer substrates cannot be inspected using transmitted-light illumination. Film thickness must be determined either by inspecting patterned features using a profilometer, or by cleaving the substrate and inspecting the film cross section in an SEM. However, silicon-wafer substrates are easier to prepare en masse than x-ray mask-blank substrates. Furthermore, due to their mechanical robustness compared to the silicon-nitride-membrane configuration of the x-ray mask, they are both easier to handle, and may be cleaved for cross-sectional examination in the SEM.

The use of glass substrates for plating experiments allowed for the use of transmitted-light bright-field microscopy on mechanically robust samples. Circular substrates of Corning "Microsheet" glass with the same diameter and approximately the same thickness as 3" silicon wafers were purchased [12]. These glass substrates were prepared with exactly the same procedure used for silicon-wafer substrates, and are compatible with the plating fixturing designed for silicon-wafer substrates. Plated-gold films on these substrates may be inspected in the optical microscope using substage illumination, and inspection of cross-sectional regions on cleaved samples in the SEM may also be performed. (Although the glass is amorphous and thus has no crystal-symmetry directions along which to cleave, it is much more manageable than

the easily-shattered silicon-nitride membrane on x-ray masks). The edge-depletion problem described above was duplicated using flex-glass substrates and photoresist patterned using conventional optical lithography.

2.2.3 Observation of "Bubble" Defects

Another observation was made on the flex-glass samples. In the plated-gold films, circular defects (of diameters on the order of 1 μm) were observed in the optical microscope using transmitted-light illumination. These circular defects resembled "bubbles" in the gold film. In some cases, there was vertical "streaking" on the film that appeared to terminate on the circular defects.

We believed that the circular defects were caused by the formation of gaseous bubbles on the surface of the cathode. At the site of bubble formation, the gold ions are physically obstructed from reaching the cathodal surface. Thus the plating reaction is effectively terminated, so long as the bubble remains attached. Figure 2-5 is a scanning-electron micrograph illustrating a bubble defect.

On some samples, possible evidence of bubble detachment was observed in the form of "streaking" on the surface of the gold film, possibly as other bubbles are dislodged.

Having found indirect evidence of gas evolution in the plated films, we attempted to directly observe and confirm bubble evolution during the plating process, by simply illuminating the set up as shown in Figure 2-6 and looking for any signs of bubbles during the reaction.

Another attempt at direct bubble observations was made by inspecting a freshly-plated sample. This sample had been removed carefully from the plating solution so that the sample remained wet with plating solution. Thus any attached bubbles would remain attached to the sample and possibly be visible in a low-magnification stereo microscope or a conventional optical microscope. In both cases, for typical current densities used in plating samples (from 0 to 0.8 mA/sq-cm), no bubbles were observed. At "higher" current densities (greater than 1 mA/sq-cm), while watching the plating reaction, a subtle disturbance to the solution was observed emanating from

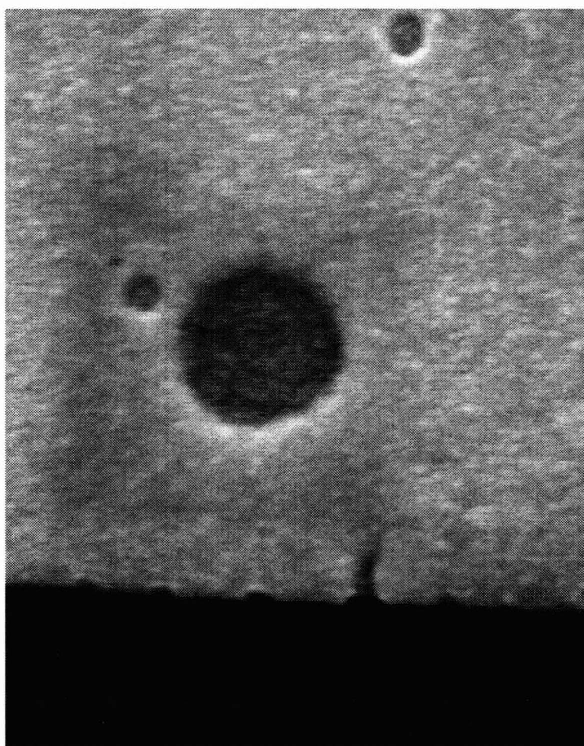

Figure 2-5: SEM photo of a possible bubble defect of diameter ~0.5 μm.

the plating fixturing, floating upwards from the sample. The disturbance resembled variations in indices of refraction in the solution, possibly corresponding to either bubbling or local heating of the solution. Furthermore, on some wafer samples after rinsing, the plated-gold film showed clear evidence of streaking emanating from the points of electrical contact between the fixturing and the sample.

Similar "bubbling" behavior was not observed in experiments using a different batch of the BDT-510 plating solution, nor were edge-depletion defects observed when using the new batch of plating solution. We believed that these "bubble" phenomena were the result of a tainted or contaminated plating solution. Replacement of the plating solution with a fresh batch minimized the observed plating problems.

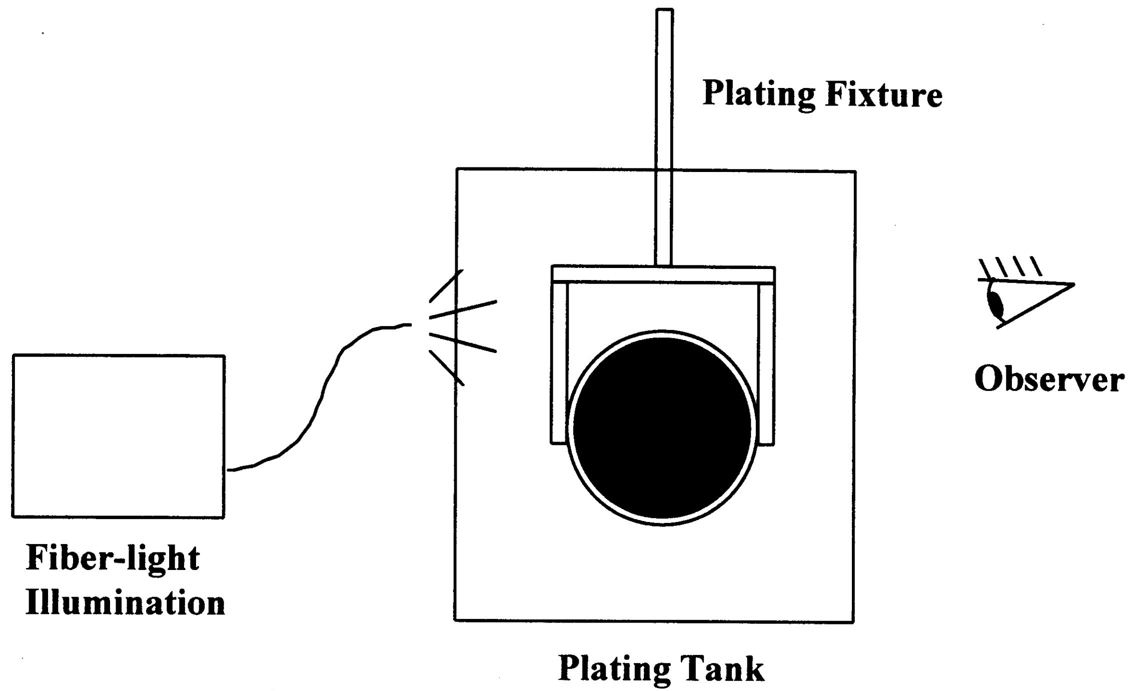

Figure 2-6: Illumination set up to attempt direct observation of bubble evolution.

Chapter 3

Electrochemistry of Gold Plating

3.1 Introduction

We studied the chemistry of the plating reaction to determine if the non-uniform "edge-depleted" plating problem described in Section 2.2.1 could be explained and solved chemically. As will be discussed, a reference electrode was used to study the plating solution and associated "brightening" agents. Although these experiments did not provide a conclusive diagnosis or solution to the "edge-depletion" problem, additional insight was gained about the plating reaction and how it may be characterized.

3.2 BDT-510 Plating Solution Chemistry

The plating solution we used was Sel-Rex BDT-510, a commercially available gold sulfite solution [13]. BDT-510 is primarily an aqueous solution of sodium aurosulfite ($Na_3Au(SO_3)_2$). In addition to the gold(I) sulfite complex, it also includes sodium sulfite (Na_2SO_3) and additional proprietary compounds added to maintain solution conductivity and pH at appropriate levels [14].

The dissociation reaction of the aurosulfite ion is described by:

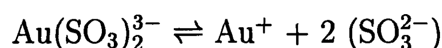

$$Au(SO_3)_2^{3-} \rightleftharpoons Au^+ + 2\ (SO_3^{2-})$$

and the electroplating half-reaction at the cathode is given by:

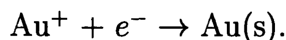

$$Au^{+} + e^{-} \rightarrow Au(s).$$

In our laboratory set-up, the electrons are provided by a regulated current source. The deposition rate is controlled by the amount of current. The tabulated current-time, measured film thickness and plating area may be used to calculate the plating efficiency, the fraction of electrons consumed by the gold-plating reaction, according to a simple plating model.

In addition to the basic gold-plating solution, BDT-510 is used with a proprietary compound called BDT Brightener. The BDT Brightener provides arsenite ions, which are incorporated into the film as arsenic [15]. The brightener limits the size of the plated gold grains by providing nucleation sites for the gold at each arsenic "impurity." This inhibits the formation of crystalline spikes or dendrites of gold, resulting in a film morphology that is smooth to the order of the gold-grain size.

The half reactions associated with the brightener include the reduction of the arsenite ion into arsenic at the cathode:

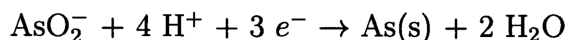

$$AsO_2^- + 4\ H^+ + 3\ e^- \rightarrow As(s) + 2\ H_2O$$

and the oxidation of arsenite into arsenate ion:

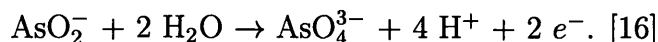

$$AsO_2^- + 2\ H_2O \rightarrow AsO_4^{3-} + 4\ H^+ + 2\ e^-.\ [16]$$

We suspected that the non-uniform plating problems might be related to the brightener. Although the use of brightener is standard for most gold-plating applications (e.g. jewelry), it was not clear if brightener was recommended for plating sub-micron features on x-ray masks. Another concern was that the plating solution might have been contaminated. In some plating runs, the plating efficiency was observed to be anomalously low (~30% or less). We suspected that the plating efficiency was low as a result of chemical reactions other than the reactions needed for gold plating. Any undesired reactions might be affecting the uniformity of the

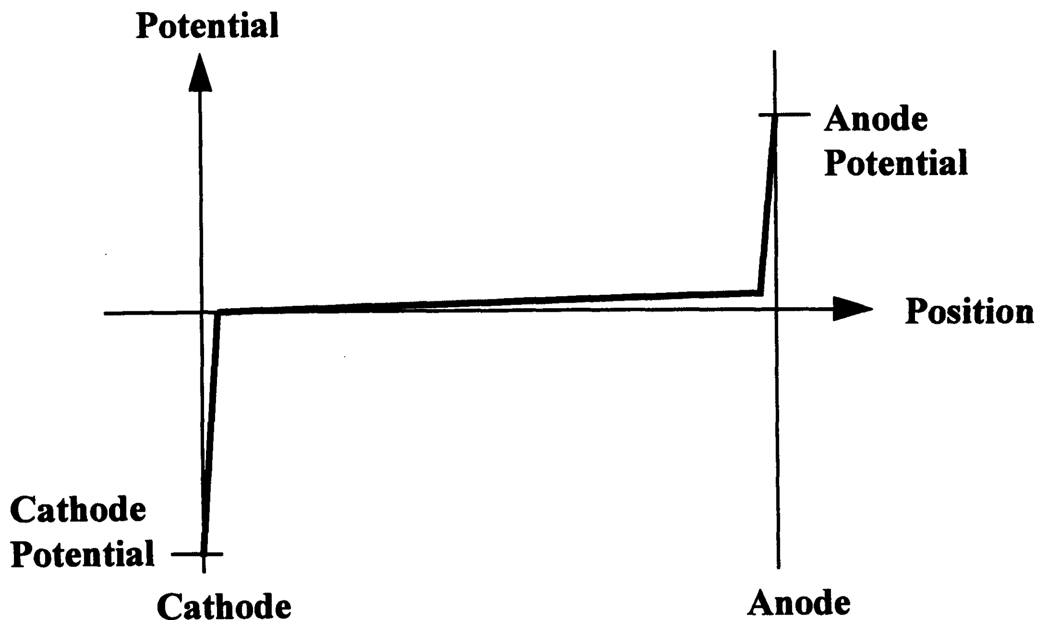

Figure 3-1: Illustration of potential distribution in a typical electroplating reaction

plated-gold film, leading to the "edge depletion" defects we had observed in the optical microscope using transmitted-light illumination (Section 2.2.1). One common reaction seen in electrochemical reactions is the reduction of hydrogen ion into hydrogen gas. It is possible that contamination in the bath might lower the threshold for hydrogen evolution, thus reducing the plating efficiency and perhaps affecting the uniformity of the plated-gold film.

3.3 Reference Electrode

In order to gain a better understanding of the electrochemical reactions occuring during the plating reaction, a saturated-calomel reference electrode (SCE) was added to the plating system. The use of a reference electrode allowed us to measure the electrochemical potentials at a given electrode with respect to the solution, and to gain insight into the reactions occuring at each electrode (Figures 3-1 and 3-2)

These measurements can potentially yield information on the effective concen-

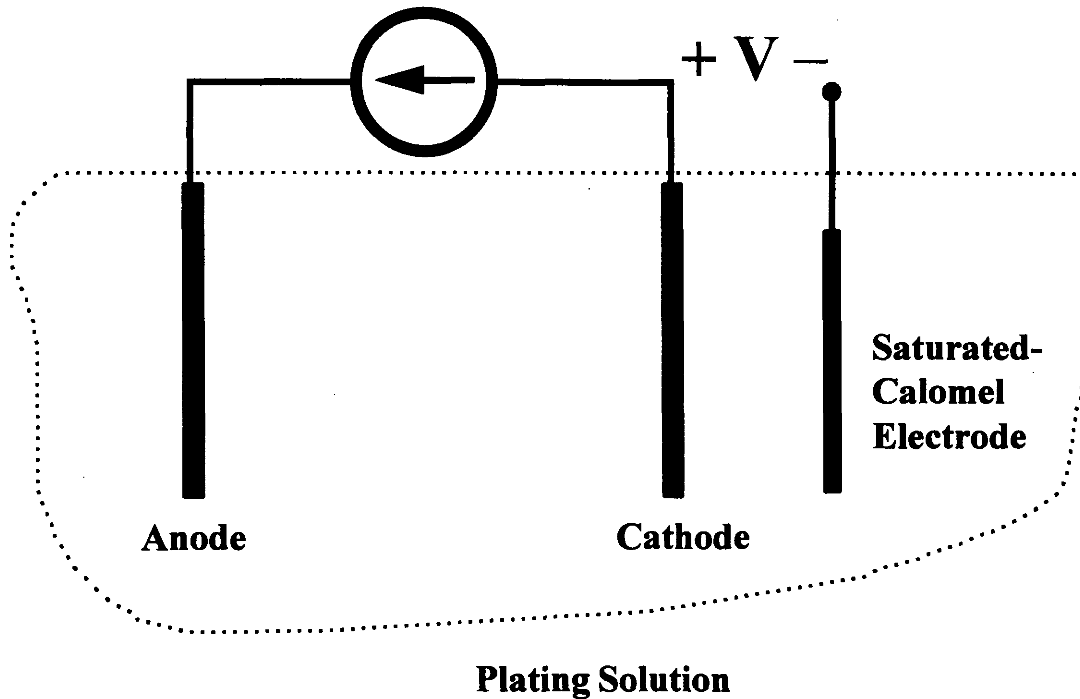

Figure 3-2: Schematic of plating circuit illustrating SCE placement

tration of brightening additives, the "quality" of the bath, and whether the plating process might be operating in a regime conducive to plating gold onto x-ray masks.

For our purposes, we concentrated on measuring the potential difference between the cathode, where the gold plating is occurring, and the SCE. The anode potential may be similarly measured.

3.3.1 Hull-Cell Measurements

A commercially-available Hull plating cell was initially used to observe the effect of BDT-Brightener concentration (and hence arsenite concentration) on the electrical characteristics of BDT-510 plating solution. A schematic diagram of a Hull cell is shown in Figure 3-3. [17]

An SCE was used to measure the cathodic potential with respect to SCE as a function of anode current. The results of this measurement are shown in Figure 3-4.

The magnitude of the cathodic potential decreases as the brightener concentration

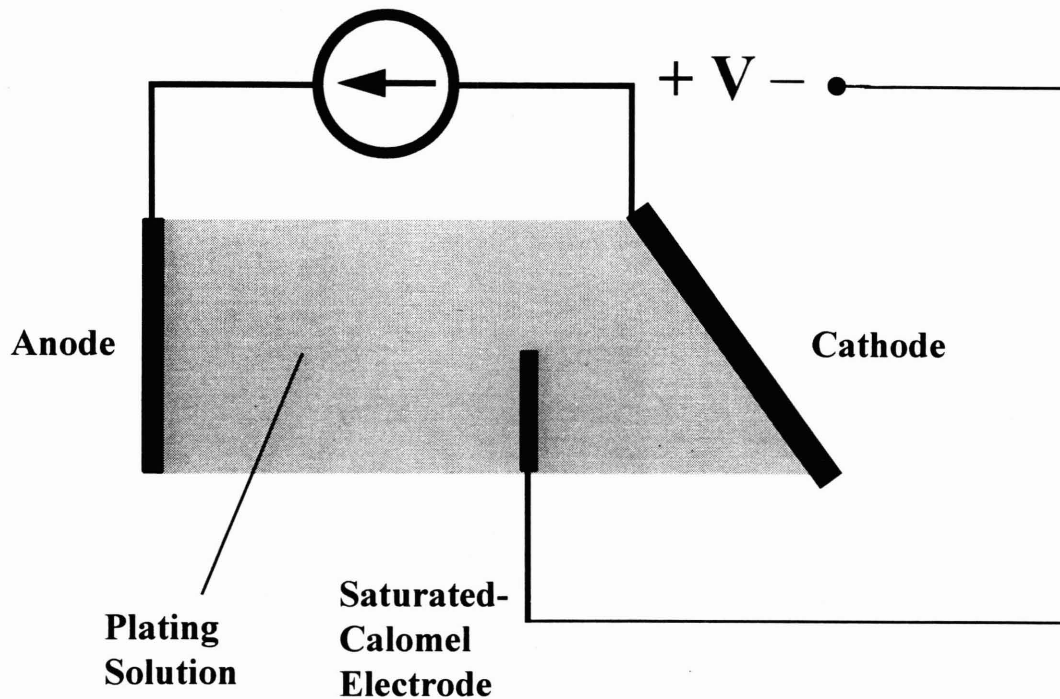

Figure 3-3: Illustration of a Hull plating cell. The geometric configuration of the Hull cell dictates the current-density distribution at the cathode.

increases, until the brightener concentration reaches a "saturation" concentration. Further addition of brightener has little effect on the cathodic potential as a function of brightener concentration.

The use of a Hull cell for the purpose of measuring the cathodic potential as a function of brightener concentration and plating-current density is not ideal. The main problem with the Hull cell in this application is that the Hull-cell geometry is designed so that the plating-current density varies over the area of the cathode surface [17]. The cathodic-potential measurement is not uniquely correlated to a plating-current density at the cathode. Furthermore, the Hull-cell measurement cannot be performed during an actual mask-plating run and must be performed separately. An in-situ measurement is preferred.

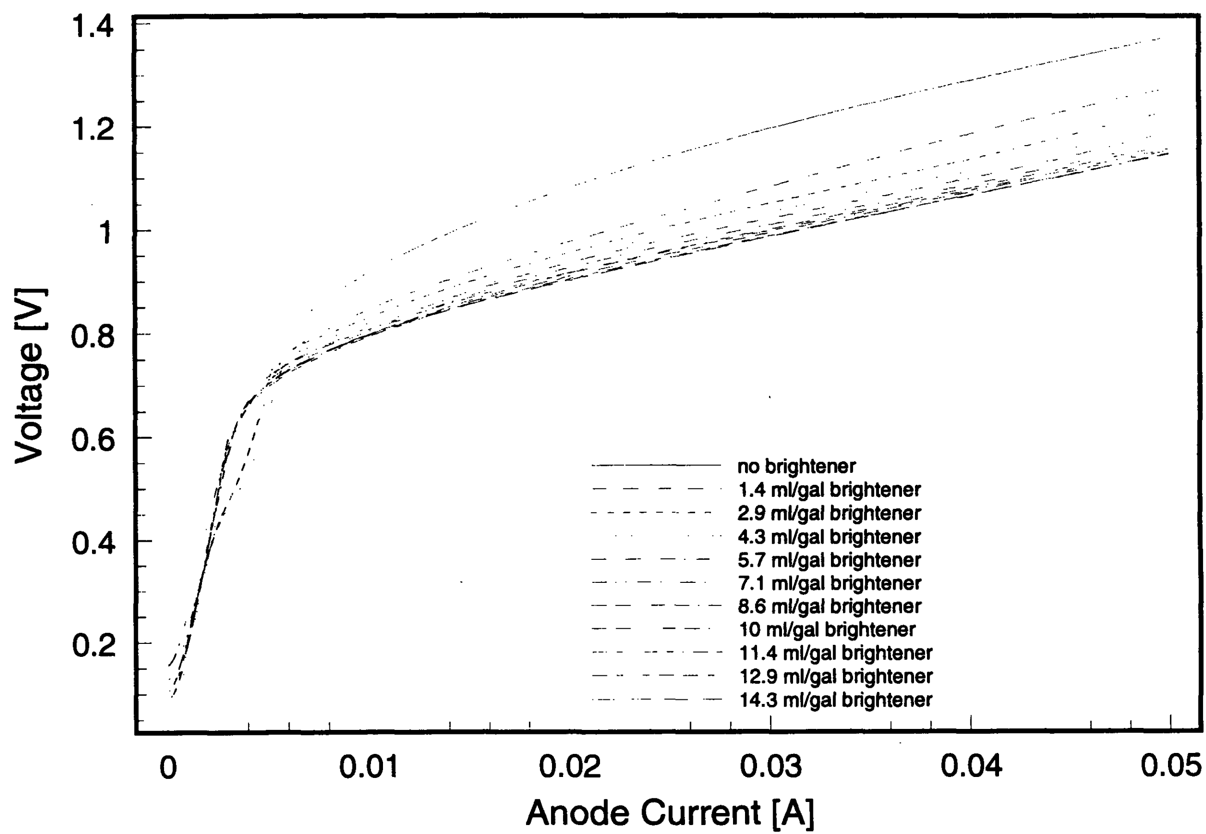

Figure 3-4: Cathodic potential, as measured by SCE, versus anode current for BDT-510 for varying BDT Brightener concentrations

3.3.2 In-situ Measurement

In the NSL plating setup, an SCE is placed in the plating solution, and the voltage between the x-ray mask (or other sample to be plated) and the SCE is measured. This voltage is the cathodic potential, with respect to the solution potential.

The placement of the SCE in the solution is not a critical parameter in this case, as the gold-plating solution is highly conductive. This was confirmed by performing a plating experiment using a silicon plating-base monitor wafer as the cathode, holding the plating current (and thus the plating-current density) constant, and measuring the cathodic potential when the SCE is placed at different positions in the plating tank. The variations in the voltage measurements were observed to be less than 0.01 V, which is sufficiently stable for our purposes. This establishes that the voltage drop in the solution can be neglected relative to the voltage drops at the electrodes.

3.4 Experimental Results

3.4.1 Varying Concentration of BDT Brightener

Measurements of the cathode potential with respect to plating-current density were performed, using the NSL plating fixturing. A silicon-wafer plating-base monitor was used as the cathode. A fresh BDT-510 plating solution was used to obtain "baseline" measurements. The concentration of BDT Brightener in the plating solution was increased between measurements. The results are shown in Figure 3-5.

For a given current-density, the cathodic potential can be correlated to the brightener concentration, suggesting a method of measuring the concentration of the brightener in the plating solution, and thus the concentration of the arsenite ion in the solution. However, it should be noted that the arsenite concentration can not be accurately determined from the measured cathodic potential without detailed knowledge of the composition of the proprietary BDT-510 plating solution and BDT Brightener.

Other researchers have developed analytical techniques to quantitatively measure the concentration of the arsenite ion in solution. These techniques require specialized

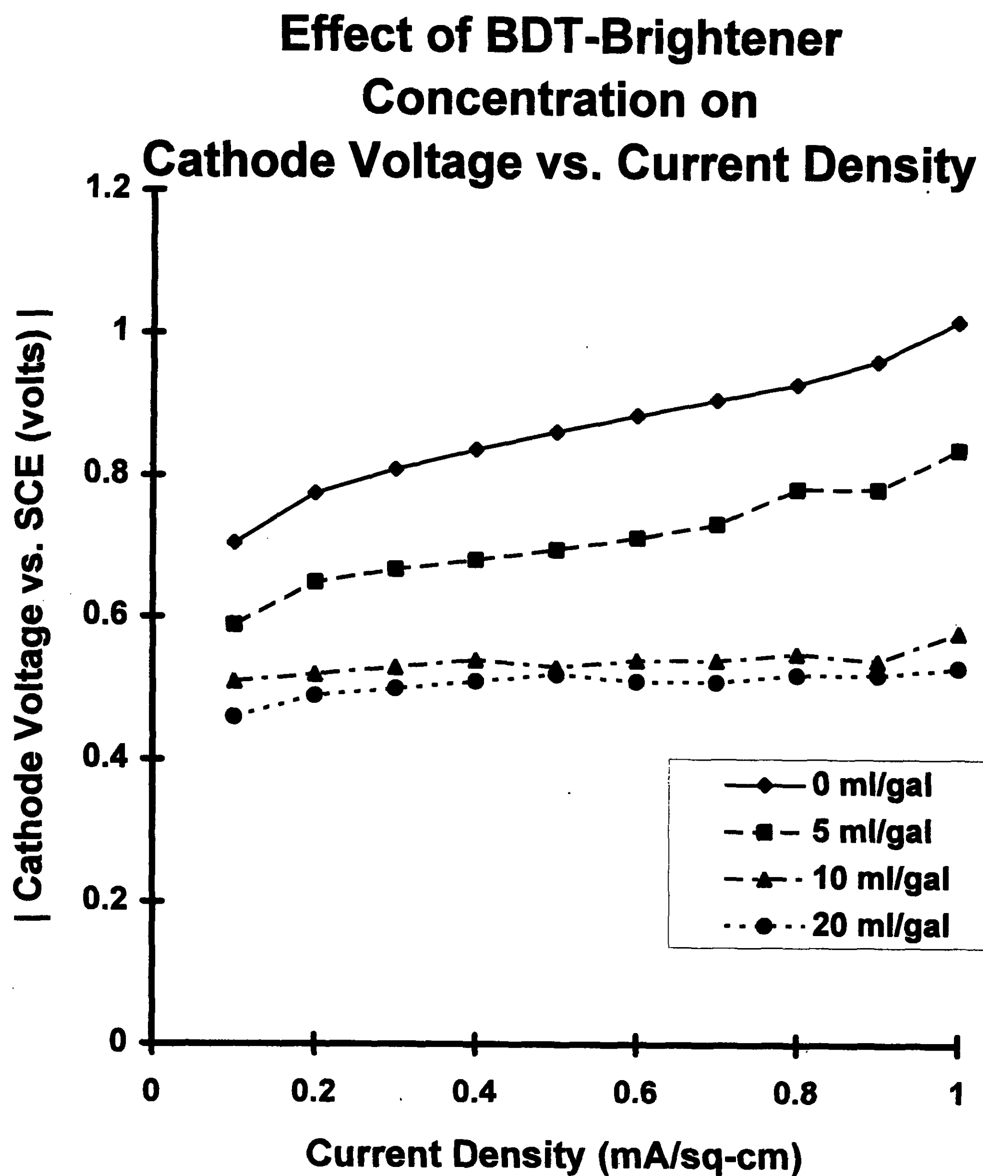

Figure 3-5: Family of curves for the cathode voltage versus current density for varying BDT Brightener concentration.

chromatographic equipment and techniques, as the presence of sulfite ions from the plating bath interferes with the measurement of the arsenite ion [18].

3.4.2 Age of Plating Bath

The behavior of the plating bath over time is another issue with respect to understanding the bath chemistry. Figure 3-6 shows the cathodic potential as a function of plating-current density for the same plating bath, taken at various times over the course of few weeks.

This solution aging occurs as a result of the dissociation reaction of the arsenite ion into arsenate ion. Also, the arsenite ion is normally plated out as arsenic to brighten the gold plate (the arsenate ion remains unchanged during the plating reaction) [15]. Futhermore, the presence of the sulfite ion catalyzes the the oxidation of the arsenite into arsenate in the ambient air of the laboratory [18]. With respect to gold plating, this means that the effective concentration of brightener decreases with time.

3.4.3 Measurement of Defective Bath

We measured the cathode potentials versus plating-current density of the "defective" plating bath to compare with the measurements of a freshly-mixed solution. Any differences in the curves are possibly related to undesired chemical reactions which might contribute to the "edge-depletion" defects described in Section 2.2.1.

The cathode voltage as a function of plating-current density of the NSL plating bath were measured and compared to the measurements of Section 3.4.1 (Figure 3-7).

For current densities less than 0.8 mA/sq-cm, the defective-NSL-plating-bath curve follows the the zero-brightener curve closely. At higher current densities, the measured cathode voltage increases in magnitude faster than the zero-brightener curve.

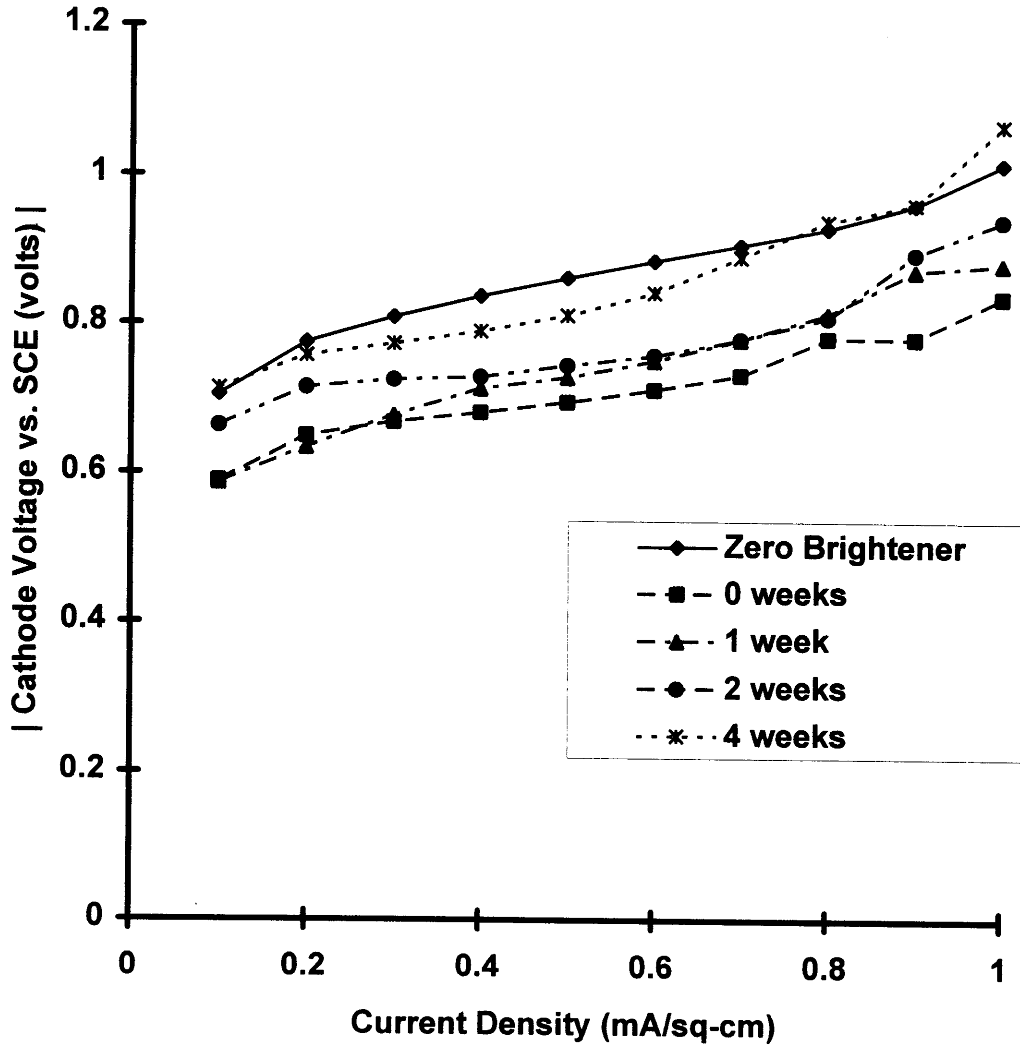

Figure 3-6: Cathode potential versus current density for different plating-bath ages. The concentration of BDT Brightener at 0 weeks is 5 ml/gallon.

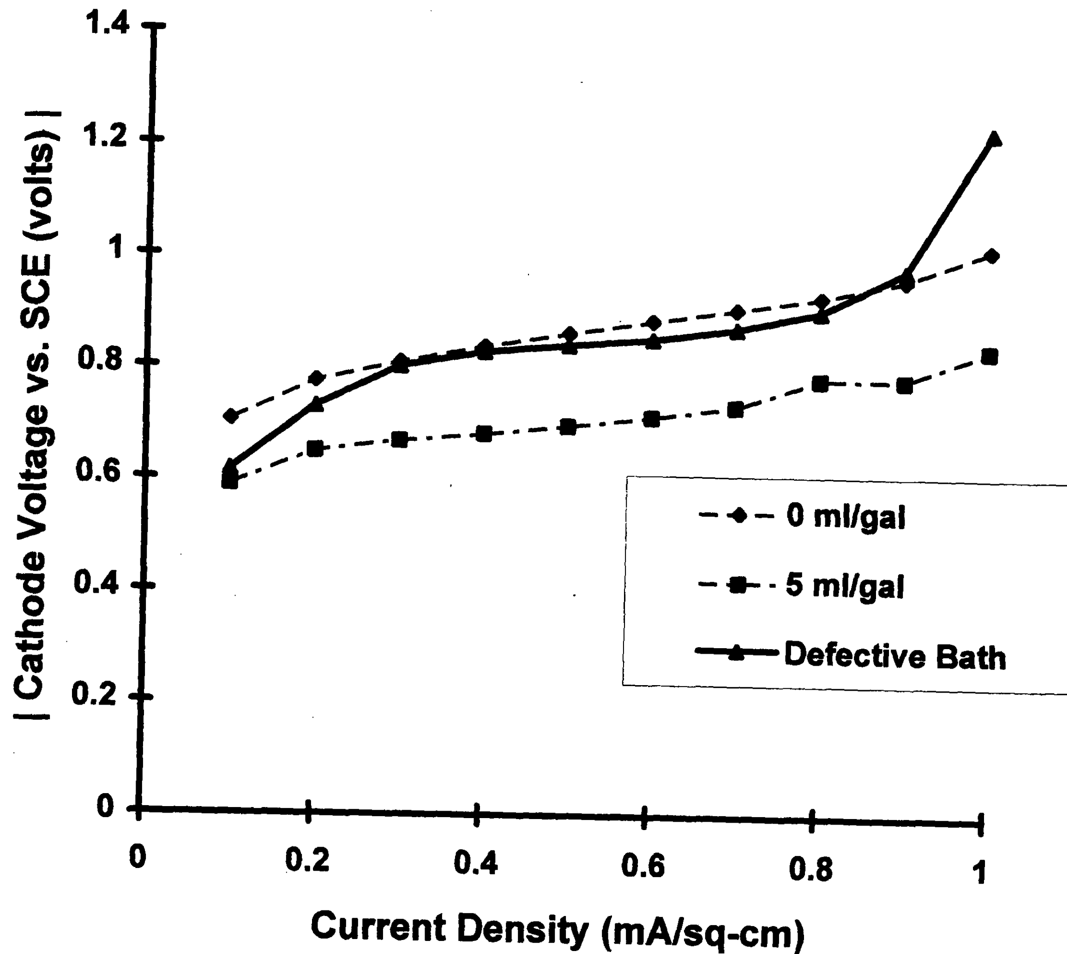

Figure 3-7: Measurement of the cathode potential versus current density for the defective plating bath. For comparison, the corresponding measurement for plating baths with 0 and 5 ml/gal concentrations of BDT Brightener are also shown.

3.5 Discussion of Measurements

According to the cathode-potential measurement, the defective-NSL-plating-bath voltages correspond to those of BDT-510 without BDT Brightener. This alone is not the problem, as can be seen in the higher-current-density behavior (around 1 mA/sq-cm). Furthermore, at various current densities from 0.2 to 1.0 mA/sq-cm, gold plated onto silicon plating-base monitor wafers using the defective NSL plating bath appeared red and less bright in scattered light, whereas gold plated using fresh BDT-510 without brightener appeared gold in scattered light, and comparatively less rough.

The electrical characteristics of the NSL bath might be explained by bath aging (and oxidation of the arsenite ion). The morphological differences between the NSL bath and BDT-510 without brightener are likely due to something other than brightener deficiency.

The relative increase in the cathode potential around 1.0 mA/sq-cm suggests that reactions other than the typical plating reaction are occurring. This is consistent with the observation of low plating efficiencies in some plating runs, and the observation of bubble-like features in some plated-gold films (described in Section 2.2.3) suggests that one component of the undesired reactions includes bubble evolution. Lacking any further information, we decided that the plating bath had been contaminated either through use or prior to acquisition from the vendor, and replaced it with a fresh bath of BDT-510.

Chapter 4

Conclusions

The problems we encountered with mask replication were found to be the result of a non-uniform plating rate in our gold films near resist edges. These "edge-depletion" defects caused the fine-gold features on our x-ray masks to be thin relative to the coarse features. As a result, there was insufficient contrast in the x-ray exposures to print the fine features from the masks. The "edge-depletion" defects were observed by inspecting the plated masks in an optical microscope and using transmitted-light illumination. The likely presence of undesired reactions was suggested by the presence of "bubble" defects. Furthermore, electrochemical measurements of the cathode-voltage behavior of the BDT-510 plating bath suggested that our problems were likely due to chemical contamination. Replacement of the plating solution from a different batch of BDT-510 was necessary.

The use of bright-field transmitted-light microscopy in conjunction with a "thickness standard" also provides a convenient method of measuring the thickness of plated films in the optical microscope, as an alternative to profilometric or interferometric methods.

Electrochemical measurements of untainted BDT-510 plating solution suggest that the active ingredient in the BDT Brightener (arsenite ion) oxidizes readily in the laboratory environment. Thus, the effective concentration of brightener in the plating bath varies according to the age of the plating bath.

This has potential implications with regards to being able to plate gold films at

"low" stress reproducibly over the lifetime of the bath, as the stress of the plated gold film depends on the amount of arsenite in the plating bath [18].

Continuing work with gold-plating technology pertaining to x-ray mask fabrication could include a study of the dependence of plated-gold film stress as functions of brightener concentration and/or bath age for the BDT-510 gold-plating solution. Another direction might include the study of alternative plating solutions. Enthone-OMI Neutronex 309 is a gold-sulfite-based plating bath that uses a thallium-based brightener and has been reported to be able to plate gold films at low stress over a wide range of brightener concentrations [19]. The addition of AC components to the current source (so-called "pulse plating") is another area that could be explored with respect to film uniformity and morphology.

Bibliography

[1] D. L. Spears and H. I. Smith, "High-resolution pattern replication using soft x rays," *Elec. Lett.*, vol. 8, pp. 192–204, 1972.

[2] M. Burkhardt, *Fabrication Technology and Measurement of Coupled Quantum Dot Devices.* PhD thesis, Massachusetts Institute of Technology, 1995.

[3] R. A. Ghanbari, *Physics and Fabrication of Quasi-One-Dimensional Conductors.* PhD thesis, Massachusetts Institvte of Technology, 1993.

[4] K. Ismail, *The Study of Electron Transport in Field-Effect-Induced Quantum Wells.* PhD thesis, Massachusetts Institute of Technology, 1989.

[5] V. V. Wong, *Fabrication of Distributed-Feedback Devices Using X-Ray Lithography.* PhD thesis, Massachusetts Institute of Technology, 1995.

[6] H. Hu, *Experimental Study of Electron Velocity Overshoot in Silicon Inversion Layers.* PhD thesis, Massachusetts Institute of Technology, 1994.

[7] A. Moel, W. Chu, K. Early, Y.-C. Ku, E. E. Moon, F. Tsai, H. I. Smith, M. L. Schattenburg, C. D. Fung, F. W. Griffith, and L. E. Haas, "Fabrication and characterization of high-flatness mesa-etched silicon nitride x-ray masks," *J. Vac. Sci. Technol. B*, vol. 9, pp. 3287–3291, 1991.

[8] M. L. Schattenburg, K. Early, Y.-C. Ku, W. Chu, M. I. Shepard, S.-C. The, H. I. Smith, D. W. Peters, R. D. Frankel, D. R. Kelly, and J. P. Drumheller, "Fabrication and testing of 0.1 μm linewidth microgap x-ray masks," *J. Vac. Sci. Technol. B*, vol. 8, pp. 1604–1608, 1990.

[9] W. Chu, *Inorganic X-ray Mask Technology for Quantum-Effect Devices.* PhD thesis, Massachusetts Institute of Technology, 1993.

[10] Scott Hector, private communication.

[11] J. H. Richardson, *Handbook for the Light Microscope: A User's Guide.* Noyes Publications, 1991.

[12] Corning Incorporated, Corning, NY 14831.

[13] Enthone-OMI, New Haven, CT 06508.

[14] Paul T. Smith, U.S. Patent #3,666,640.

[15] Phil Fusco, Enthone-OMI, private communication.

[16] M. Pourbaix, *Atlas of Electrochemical Equilibria in Aqueous Solutions.* Pergamon, 1966.

[17] R. H. Rousselot, "Current Distribution Problems: Solution by Analogical Methods," *Metal Finishing*, pp. 56–61, October 1959.

[18] Raul Acosta, IBM, private communication.

[19] W. J. Dauksher, D. J. Resnick, W. A. Johnson, and A. W. Yanof, "A New Operating Regime for Electroplating the Gold Absorber on X-Ray Masks," in *Microcircuits Engineering*, 1993.

Additional Bibliography Regarding Electroplating

Allen J. Bard and Larry R. Faulkner, *Electrochemical Methods: Fundamentals and Applications.* Wiley, 1980.

Frederick A. Lowenheim, *Modern Electroplating.* Wiley, 1974.

Ernst Raub and K. Müller, *Fundamentals of Metal Deposition.* Elsevier, 1967.

A. Vagramian, *Technology of Electrodeposition.* Teddington Draper, 1961.